© smp chair committee (Kourosh Koushan and Sverre Steen)
DOI: 10.15480/882.9307

Eighth International Symposium on Marine Propulsors
smp'24, Berlin, Germany, March 2024

# Development of an efficient CFD-based procedure with transition-sensitive turbulence model for evaluating the performance of marine propellers

**Mohamed Fathy Fouad[1], Mohamed Abbas Kotb[2], Moustafa Abdel-Maksoud[3], Moustafa Yasser Moustafa[1], Tamer Mahmoud Ahmed[2]**

[1]Egyptian Armed Forces, Egypt
[2]Alexandria University, Egypt
[3]Hamburg University of Technology, Germany

## ABSTRACT

In this paper, a CFD-based procedure for the evaluation of the performance characteristics of the well-known PPTC propeller, at model scale, is presented in detail. Results are obtained using one of the Local Correlation based Transition Models (LCTM), namely, the $\gamma - \widetilde{Re}_{\theta t}$ transition model in combination with the $k-\omega$ SST turbulence model in a RANS-based numerical procedure to predict transition over the blade surface. The aim of using the $\gamma - \widetilde{Re}_{\theta t}$ transition model is to predict the onset of transition and its influence on the propeller's overall performance and on the flow behavior. Another aim of the work is to investigate the influence of the laminar-turbulent transition on the propeller's flow. With the transition model, the constrained streamlines reflect an improvement in the flow pattern as compared to that of the model used for fully turbulent flow. Results also show an accurate prediction of the propeller's global coefficients when the transition model is applied. Finally, a comparison between the results of the different transition models is conducted showing privilege of the $\gamma - \widetilde{Re}_{\theta t}$ over other transition models in terms of predicting the overall performance of the propeller.

**Keywords**

CFD, PPTC Propeller, Transition-sensitive turbulence model.

## 1 INTRODUCTION

Nowadays and with the rapid development in computational resources, many ship hydrodynamic problems can be solved using Computational Fluid Dynamics (CFD) rather than reverting to experiments. CFD tools can accurately produce the desired results while being cost effective and time efficient as compared to experiments. In the past and for assessing, for instance, the performance of propulsion devices, experiments were the only way forward either in full or model scale. Additionally, CFD tools offer various numerical techniques for modeling flow fields about various propeller designs while also providing detailed instantaneous and local flow characteristics within the computational domain.

While turbulence models, such as the $k-\omega$ SST or the $k-\varepsilon$ model, are known to give good estimates of the developed turbulence in the flow, their applicability to estimate the hydrodynamic performance of ship propellers in model scale has some limitations since the transition mechanism from laminar to turbulent pattern cannot be considered. This shortcoming mostly leads to high discrepancies between the estimated numerical results and experimental measurements, especially at low Reynolds numbers where the flow transition is likely to have an impact. These discrepancies may be mitigated by adopting transition-sensitive models such as the $\gamma - \widetilde{Re}_{\theta t}$ transition model. The main advantage of this type of model is providing a precise evaluation and understanding of the propeller's performance characteristics under transition from laminar to turbulent flow.

A propeller blade's suction side exhibits a variety of flow patterns: a separation bubble at the leading edge, laminar flow at the inner radii followed by laminar separation -with or without- transition to turbulent flow and, turbulent flow at the outer radii.

Since the 1990s, viscous flow approaches for predicting the flow patterns about 2D profiles started to be in common use. RANS-based numerical tools were developed to simulate viscous flow patterns. RANS simulations for marine propellers were proposed by Abdel-Maksoud (2003) and Watanabe et al (2003).

Studies conducted by Felicjancik et al. (2016), Tu (2019), Nakisa et al. (2010) and Baltazar et al. (2015) played a significant role in subsequent studies for predicting propellers' open water properties using the RANS approach. However, it was not investigated whether the combination of different numerical setups and mesh types affects the performance of the turbulence models used.

In addition, it is well known that turbulence models proposed by Menter (1994) and Menter et al. (2006) were capable of giving proper estimates of the developed turbulent flows but were incapable of predicting the transition mechanism from laminar to turbulent pattern. Additionally, the turbulence models $k-\omega$ SST and

$k-\varepsilon$ are not sensitive to variations in the turbulence quantities imposed at the computational domain's inlet, as these models can capture and predict fully developed turbulent flows but are not able to simulate flow transitions. This highlighted the importance of adopting transition sensitive models.

RANS turbulence models are intended for high Reynolds numbers. In the initial stages of transition modeling, the Large Eddy Simulation (LES) model was developed to capture the flow including the transitional effects, especially at moderate Reynolds numbers for practical flows. However, LES models require high computational resources (Spalart & Rumsey 2007). LES still needs appropriate specifications of the turbulence free-stream definition and external disturbance if they are adopted within the modeling. Another obstacle that arises with the LES model is its sensitivity to the sub-grid scale model which was discussed by Lardeau et al. (2012).

Similarly, the Direct Numerical Simulation (DNS) model suffers from the same shortcomings regardless of its optimum performance for some transition flows which was reported by Savill (2002).

Extensive research has been conducted to forecast the propellers' performance utilizing transition-sensitive turbulence models. This included the three equations eddy viscosity turbulence model $k-k_L-\omega$ conducted by Wang & Walters (2012) and Helal et al. (2018). The turbulent laminar kinetic energy model $k_l$ was introduced by Mayle & Schulz, (1971). It revealed the progression of the laminar energy fluctuation during transition before the boundary layer transition. This led to better agreement between experimental and numerical results.

The fundamental implication of RANS is that the linear amplitude of the disturbances is eliminated by an averaging process and the discarded linear effects may appear to be not consistent with transition physics. In addition, the shape of the propeller or the flow separation points disperses the laminar to turbulent transition because it happens in such a limited flow zone. Nevertheless, a RANS-based CFD code can capture these effects by implication of appropriate correlations in the code. The output of those implications between the RANS model, the transition models, and the appropriate correlation is the Local Correlation-based Transition Model (LCTM).

This model does not model the physics of the flow but identifies the region of the flow where the laminar to turbulent transition occurs. All physics involved is modeled by empirical correlations in which a unique transition mechanism is taken into account. While the LCTM approach is different compared to other transition models which are based on Linear Stability Theory, nevertheless, it is still one of the best suited models to capture the laminar to turbulent transition regions (Ingen 1956).

As a result of the previous challenges, the LCTM has generated different transition models: such as the Gamma ReTheta transition model $\gamma-\widetilde{Re}_{\theta t}$ ,developed by Langtry (2006) and improved later by Langtry & Menter (2009), which became the most appropriate model for the simulation of transition flow on marine propellers. This model is based on two supplementary transport equations, one for the intermittency, which was proposed by Narasimha (1957) and the other equation is for the transition onset momentum thickness Reynolds number.

The second transition model is the Gamma model, $\gamma$, which was developed by Menter et al (2015). This intermittency equation is merged with the $k-\omega$ SST model proposed by Menter (1994) and Menter et al. (2003) to predict and mimic the flow about the propeller including the transition mechanism due to free-stream turbulence intensity and pressure gradient.

Based on the above-mentioned studies, this paper will adopt the $k-\omega$ SST model, with and without the $\gamma-\widetilde{Re}_{\theta t}$ model, to accurately predict the propeller performance, to investigate the influence of transition on the propeller flow and, to study the transition and related physics.

## 2 THEORITICAL ANALYSIS AND MATHEMATICAL MODEL

In this work, the computations are carried out using the commercially available code STAR-CCM+ version 2022.1. The focus in the study is to investigate the ability of $\gamma-\widetilde{Re}_{\theta t}$ transition model to predict transition over the propeller's blade surface and to determine the influence of the transition on the flow behavior and propeller performance.

### 2.1 RANS Equations

Although it is theoretically feasible to use large eddy simulation (LES) and direct numerical simulation (DNS) to fully characterize the exact turbulence solution of the Navier-Stokes Equations, this is not practical due to the high processing cost involved. Solving for averaged (or filtered) quantities and approximating the impact of minor fluctuating structures is a widely accepted technique that requires less work. This method, which makes use of turbulence models, is known as a Reynolds-averaged Navier-Stokes (RANS) technique. These models provide closure to the RANS equation and are an approximate representation of the physical phenomena of turbulence (Gray-Stephens et al. 2020).

Most engineering applications are regarding turbulent flows they need special treatment in this regard. Turbulent flows are unsteady which means that the change of velocity over time is random at most points in the flow. Turbulent flows cause an increase in diffusion called turbulent diffusion. Subsequently, friction forces on any represented body increase, as well as the power required for propulsion. A RANS method is based on equations obtained by averaging the equations of motion over time for statistically steady flows. However, these equations do not generate a closed set, hence, turbulence models are needed such as the $k-\omega$ or the $k-\varepsilon$ model.

### 2.2 Local Correlation-Based Transition Modeling

The local correlation-based transition models are the Gamma model $\gamma$ proposed by Menter et al. (2015) and the Gamma ReTheta transition model proposed by Langtry & Menter (2009).

The Gamma ReTheta transition model is based on two transport equations merged with the turbulent model kinetic energy $k$ and specific dissipation rate $\omega$. The first transport equation is intermittency, $\gamma$ which is used to activate the production of the turbulent kinetic energy downstream of the transition point inside the boundary layer (BL). The intermittency value is 1.0 in the free-stream direction to prevent any interference with the turbulence model in the free-stream area. If a different value of the intermittency is selected other than the one in the free-stream zone, this may affect the decay of the turbulence value on the inflow region of the propeller and at the beginning of the boundary layer, that also needs a stagnation point for transition which affecting the transition physics.

The transport equation for the transition momentum thickness Reynolds number, $\widetilde{Re}_{\theta t}$, is used to model the transfer of the non-local quantities such as turbulence intensity, *Tu* and the pressure gradient from the free-stream zone, and so transfer it into the boundary layer to trigger the transition.

Neither $\gamma - \widetilde{Re}_{\theta t}$ transition model nor $\gamma$ transition model can capture the transition physics through their transport equations. The transition physics is contained in the empirical correlations within the model formulation (Rubino 2022). In addition to that, the Gamma ReTheta transition model and the Gamma transition model are preferable for the bypass transition and the low turbulence intensity free-stream transition.

### 2.3 Case Study

The case study presented here is a controllable pitch propeller designed by the Potsdam Model Basin (SVA Potsdam) to evaluate the propeller open water characteristics (Heinke 2011). The performance of the model propeller PPTC VP1304 was investigated in the SVA Potsdam towing tank in homogenous flow.

Thrust $(t)$ and torque $(Q)$ are typically used to evaluate the performance of a propeller. They are expressed as non-dimensional coefficients as a function of the advance coefficient which is basically a non-dimensional form of speed. The advance coefficient J, as well as $k_t$ and $k_Q$, are defined in Equations (1) to (3)

$$k_t = t / \rho n^2 D^4 \quad \textbf{(1)}$$

$$k_Q = Q / \rho n^2 D^5 \quad \textbf{(2)}$$

$$\eta = ( k_t J ) / ( k_Q 2\Pi ) \quad \textbf{(3)}$$

The main particulars of the propeller are shown in Table 1.

**Table 1: PPTC VP1304 Particulars.**

| Particulars | Symbols | Value |
|---|---|---|
| Propeller Dimeter | D | 250 mm |
| Pitch ratio | P0.7 / D | 1.635 |
| Pitch at r/R=0.75 | $P_{0.75}$ | 407.380 mm |
| Chord at r/R=0.75 | $C_{0.75}$ | 106.347 mm |
| Thickness at r/R =0.7 | $T_{0.75}$ | 307916 mm |
| Blade area ratio | $A_E / A_o$ | 0.77896 |
| Skew | | 18.83 degree |
| Hub diameter ratio | d h / D | 0.3 |
| Number of blades | Z | 5 |
| Revolutions per second | n | 15 |
| Scale | - | 1: 1 |

### 2.5 Computational Domain Dimensions

A cylindrical calculation domain is considered for the simulations, as shown in Fig. 1. While the inlet is placed at a distance of 5D upstream of the propeller plane,(1.25 meter), the outlet is located at a distance of 13D downstream,(3.25 meter). In the radial direction, the domain diameter is extended up to a distance of 6D, (1.5 m).

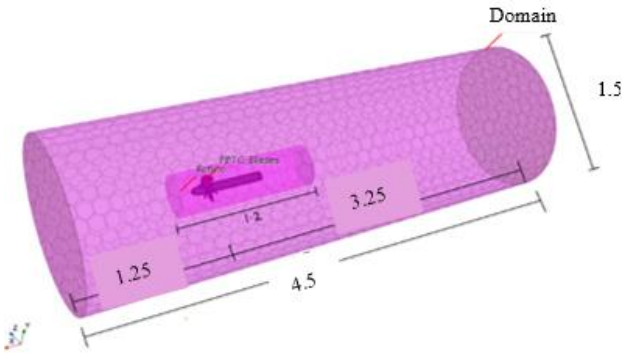


**Figure 1: Propeller Computational Domain.**

The computations are conducted for one blade as shown in Fig. 2. The interaction with the other blades is considered by imposing the periodic interfaces boundary condition on the two side surfaces. It should be noted that the periodicity applied is a rotational periodicity. The periodic domain is a 72 deg cylindrical segment with an 0.625 m radius which is 2.5D times the propeller's diameter.

All the boundary conditions imposed are shown in Fig. 2. For the stationary region (the outer surface of the periodic domain), the governing equations are solved in a fixed frame of reference, while for the rotating regions (propeller blade, hub, and fluid zone), the governing equations are solved in a rotating frame of reference.

The domain boundary condition defined at the inlet is the inflow velocity. The outer surface of the domain is defined as a slip wall while the two sides of the periodic domain are defined as interface surfaces, as mentioned before. The propeller blade is defined as a no slip wall and the shaft is defined as a slip wall, see Fig. 2.

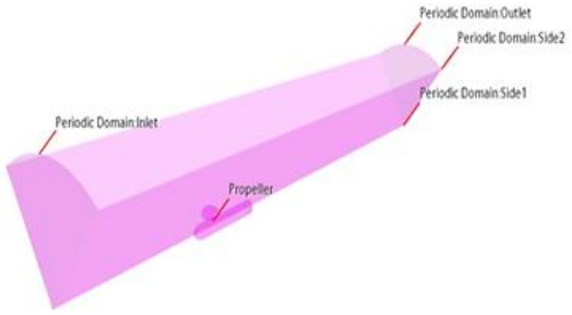


**Figure 2 :Periodic Domain Boundary Conditions.**

### 2.6 Numerical Simulation

As mentioned above, the Potsdam Propeller Test Case (PPTC) VP1304 geometry is used in the present study. Simulation results are compared with experimental data provided by SVA (Heinke 2011) with steps of 0.2 at various advance coefficients J ranging from 0.7985 to 1.4594. The propeller's rotation is kept constant at n = 15 rps. Advance velocity $V_A$ is changed by adjusting J.

The performance of the propeller is predicted using the turbulence model $k-\omega$ SST. The transition-Sensitive turbulence model $\gamma-\widetilde{Re}_{\theta t}$ is adopted to assess the calculated results. In addition, the intermittency, transition momentum thickness Reynolds number is considered, and the streamlines distribution are calculated over the blade surface to predict the flow separation and the onset of transition.

To apply the $\gamma-\widetilde{Re}_{\theta t}$ transition model to the open water propeller test simulations, some recommendations and guidelines should be applied to be able to accurately predict the transition and the propeller's performance. These recommendations are imposed onto the setup where the most important being the wall distance Y+ value which should lie between 0.1 and 1.0. The free- stream edge condition for the $\gamma-\widetilde{Re}_{\theta t}$ transition model needs to be defined. In addition, the inlet boundary conditions to control the turbulence intensity and the turbulent viscosity ratio must be specified.

The free-stream edge location must be defined since the $\gamma-\widetilde{Re}_{\theta t}$ transition model is a semi-local correlation-based model which depends on the transition onset momentum thickness Reynolds number $Re_{\theta t}$ in the free-stream. This free-stream value is transferred into the boundary layer through the transition momentum thickness Reynolds number, $\widetilde{Re}_{\theta t}$. To define the value of $Re_{\theta t}$ through the LCTM, the free-stream edge location is determined using the STAR-CCM+ field functions option. The free-stream edge is defined in Equation 4 as follows.

$$\${WallDistance}>=0.003\ ?\ 1.0:\ 0.0 \quad \textbf{(4)}$$

Where, the Field Function value is 1.0 in the free-stream and is 0.0 inside the boundary layer and, the thickness of the boundary layer is 0.003m according to the defined mesh setup.

The inlet turbulence intensity specifications are mandatory to be defined to have a good transition prediction. This turbulence intensity can decay rapidly depending on the inlet eddy viscosity ratio, $\mu_t/\mu$. As a result, the local turbulence intensity downstream of the domain inlet will be smaller than that imposed on the domain inlet. As the inlet viscosity ratio goes up, the turbulent decay rate goes down in the downstream direction. This value should be monitored precisely since a large viscosity ratio at the inlet will lead the skin friction coefficient to deviate from the laminar pattern.

To overcome this problem, a location within the simulation domain just before the propeller and away from the domain inlet must be defined which is named herein after Decay Distance. This location functions as a guide point for the controller in the streamwise direction where before it, the controller will be active, and the value of the turbulent kinetic energy and the specific dissipation rate are calculated according to Equations (6) and (7). Beyond this location, the values of the turbulent kinetic energy and the specific dissipation rate are calculated according to the normal $k-\omega$ SST formula as follows:

$$Decay\ Distance = 0.675$$

And the controller equation is defined in Equation (5) as

$$\$\${Centroid}[0]>=\${Decay\ Distance}\ ?\ 1.0:\ 0.0 \quad \textbf{(5)}$$

This is interpreted as the flow is controlled to go streamwise in the X direction which is defined as [0] in STAR-CCM coordinate system, for a horizontal distance equal to 0.675 meter. If this distance is greater than or equal to the {Decay Distance}, so the controller equals 1.0 or else equals 0.0.

The turbulent kinetic energy source equation and the specific dissipation rate source codes are defined as:

*0.09*997*${TurbulentKineticEnergy}*${SpecificDissipation Rate}*($${Centroid}[0]>=${Decay Distance} ? 1.0 : 0.0 )* **(6)**

*.0828*pow(${SpecificDissipationRate},2)*997*($${Centroid }[0]>=${Decay Distance} ? 1.0 : 0.0 )* **(7)**

The values of the turbulence intensity and the turbulent viscosity ratio for the inlet of the computational domain are set to 0.02 and 10, respectively.

## 3 RESULTS AND DISCUSSION

A comparison between the CFD results and the open-water experimental data has been conducted to validate the CFD model within the specified range of the advance coefficients (from J=0.798 to 1.459). Results presented later will be used to interpret the predictions of the propeller's performance coefficients, as well as the flow field about the propeller blade and the transition prediction.

Table 2 shows a comparison between the experimental and the numerical results for the propeller performance characteristics. The calculations are conducted using

different transition models: Gamma ReTheta, gamma transition and turbulent suppression. As it can be observed, the propeller's performance predicted by Gamma ReTheta transition model is closer to the experimental results compared with the corresponding values obtained by the gamma transition and turbulent suppression transition models.

**Table 2: Comparison of the Results of Different Transition Models.**

| | | | Transition Models | | |
|---|---|---|---|---|---|
| | J | Exp | Gamma ReTheta | Gamma | Turbulent Suppression |
| $k_t$ | 0.799 | 0.505 | 0.524 | 0.511 | 0.510 |
| | 1.068 | 0.354 | 0.374 | 0.356 | 0.359 |
| | 1.202 | 0.280 | 0.297 | 0.287 | 0.286 |
| | 1.459 | 0.139 | 0.143 | 0.138 | 0.136 |
| $10k_Q$ | 0.799 | 1.184 | 1.261 | 1.252 | 1.254 |
| | 1.068 | 0.910 | 0.965 | 0.957 | 0.959 |
| | 1.202 | 0.768 | 0.805 | 0.809 | 0.81 |
| | 1.459 | 0.494 | 0.487 | 0.492 | 0.492 |
| $\eta$ | 0.799 | 0.542 | 0.529 | 0.518 | 0.517 |
| | 1.068 | 0.661 | 0.658 | 0.639 | 0.637 |
| | 1.202 | 0.697 | 0.705 | 0.678 | 0.674 |
| | 1.459 | 0.655 | 0.683 | 0.652 | 0.643 |

### 3.1 Prediction of the Performance coefficients

In this section, the calculated thrust and torque coefficients as well as the propeller efficiency are presented. The calculations are conducted using the $k-\omega$ SST turbulence model with and without wall function and with and without $\gamma - \widetilde{Re}_{\theta t}$ transition model. The comparison is performed over a range of advance ratios from 0.7985 to 1.4594 and for the following cases:

Case 1: $k-\omega$ SST turbulence model using Y+ $< 1.0$,
Case 2: $k-\omega$ SST turbulence model using Y+ $>$ 30.0,
Case 3: $k-\omega$ SST turbulence model with activating the $\gamma - \widetilde{Re}_{\theta t}$ transition model using Y+ $< 1.0$.

Fig. 3. Shows a comparison between the experimental and the numerical results for the previously mentioned cases.

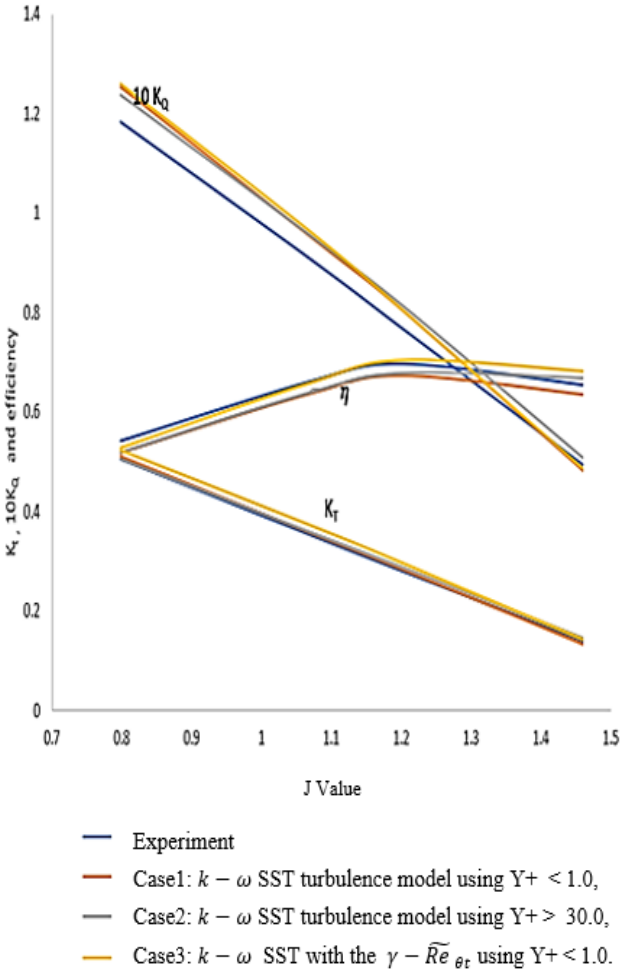


**Figure 3: Comparison of the Experimental and Numerical Results.**

Furthermore, a comparison of the calculated and measured coefficients is given in Table 3 for the different advance coefficients. The relative difference in percentage is included with respect to the experimental results.

It may be noted from Fig. 3 and Table 3 that, in general, a good agreement is achieved between the experimental data and the predicted coefficients and efficiency.

**Table 3: Experimental and Numerical Coefficients.**

| | J | Exp | Turbulence model Y+ < 1.0 | Turbulence model Y+ > 30.0 | Transition model. Y+ < 1.0 |
|---|---|---|---|---|---|
| $k_t$ | 0.799 | 0.505 | 0.51 | 0.505 | 0.523 |
| | Relative difference % | | -0.950 | -0.009 | -3.622 |
| | 1.068 | 0.354 | 0.357 | 0.354 | 0.374 |
| | Relative difference % | | -0.763 | -1.611 | -5.568 |
| | 1.202 | 0.280 | 0.282 | 0.288 | 0.296 |
| | Relative difference % | | -0.824 | -2.968 | -6.006 |
| | 1.459 | 0.139 | 0.131 | 0.146 | 0.143 |
| | Relative difference % | | 5.667 | -4.735 | -2.582 |
| $10k_Q$ | 0.799 | 1.184 | 1.253 | 1.238 | 1.260 |
| | Relative difference % | | -5.906 | -4.553 | -6.498 |
| | 1.068 | 0.910 | 0.954 | 0.957 | 0.965 |
| | Relative difference % | | -4.881 | -5.156 | -6.090 |
| | 1.202 | 0.768 | 0.803 | 0.813 | 0.805 |
| | Relative difference % | | -4.676 | -5.979 | -4.872 |
| | 1.459 | 0.494 | 0.481 | 0.508 | 0.487 |
| | Relative difference % | | 2.609 | -2.851 | 1.497 |
| $\eta$ | 0.799 | 0.542 | 0.517 | 0.518 | 0.528 |
| | Relative difference % | | 4.594 | 4.280 | 2.490 |
| | 1.068 | 0.661 | 0.635 | 0.638 | 0.658 |
| | Relative difference % | | 3.857 | 3.343 | 0.393 |
| | 1.202 | 0.697 | 0.675 | 0.678 | 0.705 |
| | Relative difference % | | 3.529 | 2.668 | -1.147 |
| | 1.459 | 0.655 | 0.635 | 0.668 | 0.682 |
| | Relative difference % | | 3.1297 | -2.061 | -4.218 |

Additionally, it can be observed from Fig. 3 and Table 3 that, higher coefficient values are obtained when the $\gamma - \widetilde{Re}_{\theta t}$ transition model is used. For the thrust coefficient, the values calculated using the $\gamma - \widetilde{Re}_{\theta t}$ transition model are higher by 3.6 % at J = 0.7985 to 6.1 % at J = 1.2021 than the measured values, while with $k-\omega$ SST turbulence model the deviation is 0.009 % for J = 0.7985 to 2.96 % for J = 1.2021. Also, the calculated values of the torque coefficient with the transition model are higher than those by using the turbulence model for J values from 0.7985 to 1.2021. Finally, the efficiency calculated using the $\gamma - \widetilde{Re}_{\theta t}$ transition model is higher than that of the $k-\omega$ SST turbulence model only.

At the higher advance ratio of 1.4594, the $\gamma - \widetilde{Re}_{\theta t}$ transition-sensitive turbulence model demonstrates a slight advantage over the $k-\omega$ turbulence model with respect to the measured results.

### 3.2 Prediction of the Flow Field about the Propeller

In this section, predictions of the propeller's flow field, based on the $\gamma - \widetilde{Re}_{\theta t}$ transition model, at different advance ratios are presented. The pressure distribution and skin friction coefficients over the blade suction side are also illustrated. The constrained streamlines for both the turbulence model and the transition model are interpreted at different advance ratios.

As discussed earlier, the influence of the values of the turbulence inlet quantities should be controlled since turbulence quantities will decay along the flow direction and the inlet values may differ at the propeller's blade plane from the initial values at the inlet boundary condition. The influence of the turbulent kinetic energy source may be monitored by placing it upstream of the propeller blade plane.

For simulations with the turbulence model $k-\omega$ SST, the inflow turbulence intensities are 1.0% and the eddy viscosity ratio $\mu_t / \mu$ is 1.0 while for simulations with the transition model $\gamma - \widetilde{Re}_{\theta t}$, the inflow turbulence intensities are 2.0 % and the eddy viscosity ratio $\mu_t / \mu$ is 10.0 for all advance coefficients.

To identify which inlet values for the $Tu$ and the $\mu_t / \mu$ should be considered at the domain inlet for numerical simulations of transitional flows, a comparison between various turbulence quantities for the turbulence model $k-\omega$ SST is carried out for $Tu$ = 1.0% and $\mu_t / \mu$ =1.0 and, $Tu$ = 2.5% and $\mu_t / \mu$ =500 which shows a strong reduction at the first instance corresponding to a small value of the $\mu_t / \mu$. In addition, a comparison between various turbulence quantities for the transition model $\gamma - \widetilde{Re}_{\theta t}$ are made for $Tu$ = 1.0% and $\mu_t / \mu$ =1.0 and, $Tu$ = 2.5% and $\mu_t / \mu$ =500, which shows similar turbulence intensity characteristics as noticed in contrast with the $k-\omega$ SST turbulence model. As the inlet is positioned 1.25 meters upstream from the position of the propeller, which is five times the diameter of the propeller, a large $\mu_t / \mu$ value is mandatory to maintain the rate of decay of the inlet turbulence intensity (Baltazar et al. 2018). Accordingly, values of the turbulence quantities of $Tu$ = 1.0% and $\mu_t / \mu$ =1.0 for the $k-\omega$ SST turbulence model and, $Tu$ = 2.0% and $\mu_t / \mu$ =10.0 for the $\gamma - \widetilde{Re}_{\theta t}$ transition model are used.

Visualization of the constrained streamlines is very useful for assessing the irregularities related to the predicted flow. The constrained streamlines are studied for the turbulence model $k-\omega$ SST and the transition model $\gamma - \widetilde{Re}_{\theta t}$ at different advance coefficients. Firstly, the constrained streamlines distribution over the blade suction side for the turbulence model $k-\omega$ SST, without activating the transition model, shows a circumferential distribution in the chord-wise direction with fully turbulent flow indicating no separation at all advance coefficients. This may be observed in Fig. 4.

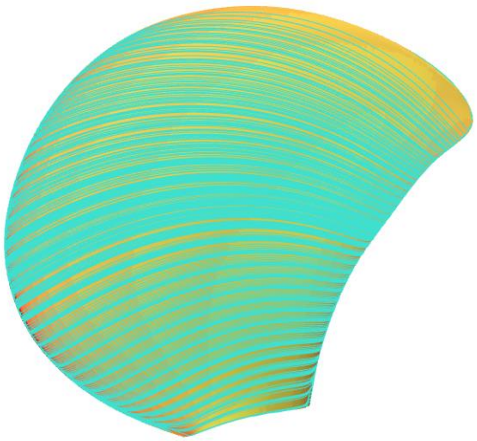

**Figure 4: Constrained Streamlines on the Suction Side with the Turbulence Model at Advance Coefficients J = 0.7985 to J= 1.4594, $Tu$ = 1.0% and $\mu_t$ / $\mu$ =1.0.**

Furthermore, the constrained streamlines distribution over the blade suction side for the transition model, $\gamma - \widetilde{Re}_{\theta t}$, at different advance coefficients and for different simulation times are shown in Fig. 5.

During the simulations, the time step is changed by three times:

- The first time-step value is (1/ rps = 1/15 = 0.066 seconds), in this case, the propeller rotates one complete revolution at each time-step. This means that the propeller blades maintain their position during the simulation despite the rotation of the propeller. The simulation is conducted for physical time of 2 seconds with an inlet velocity of 3 m/s and rotation speed of 15 rps resulting in an advance coefficient J=0.7985.
- The second time step value is (1/ (5*rps) = 1/75 = 0.0133) which means that the propeller will rotate in a manner that each blade will take the position of the adjacent blade. This is conducted for the physical time (of 2.0 seconds to 3.0 seconds.
- The third time step value is a value smaller than the previous values, at (1/ (10*rps) = 1/150 = 0.0066). The physical simulation time considered in this case is 7 seconds (from second 3.0 to second 10.0).

As it can be seen in Fig. 5, an increase in the separation area is predicted near the trailing edge of the suction side of the blade where, a change of the orientation of the streamlines occurs due to the transition observed which takes place at high value of the advance coefficients. Additionally, and by comparison, the $\gamma - \widetilde{Re}_{\theta t}$ transition model is more appropriate for predicting the constrained streamlines at the radial location of r/R $\leq$ 0.7 due to the low local Reynolds number. In contrasts, at larger radius ratios, the turbulence $k - \omega$ SST model is more applicable as the Reynolds number in this region is high.

| | |
|---|---|
| J = 0.7985 , Time-step = 1/rps<br>$T_u$ = 2.0 % , $\mu_t$ / $\mu$ =10.0<br>Simulation time 2.0 S | J = 0.7985 , Time-step = 1/(5*rps)<br>$T_u$ = 2.0 % , $\mu_t$ / $\mu$ =10.0<br>Simulation time 3.0 S |
| 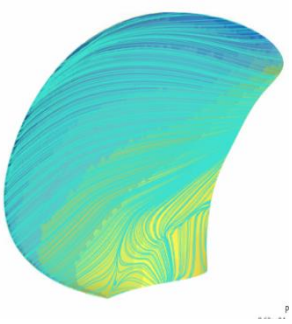 | 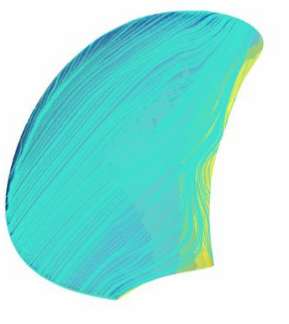 |
| J = 0.7985 , Time-step = 1/(10*rps)<br>$T_u$ = 2.0 % , $\mu_t$ / $\mu$ =10.0<br>Simulation time 4.0 S | J = 1.0683 , Time-step = 1/(10*rps)<br>$T_u$ = 2.0 % , $\mu_t$ / $\mu$ =10.0<br>Simulation time 6.5 S |
| 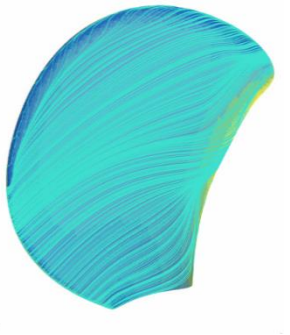 | 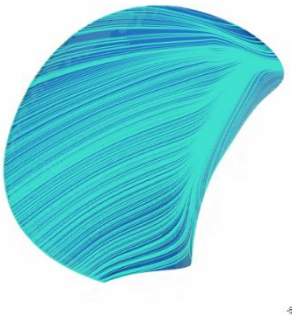 |
| J = 1.2021 , Time-step = 1/(10*rps)<br>$T_u$ = 2.0 % , $\mu_t$ / $\mu$ =10.0<br>Simulation time 8.0 S | J = 1.4594 , Time-step = 1/(10*rps)<br>$T_u$ = 2.0 % , $\mu_t$ / $\mu$ =10.0<br>Simulation time 10.0 S |
| 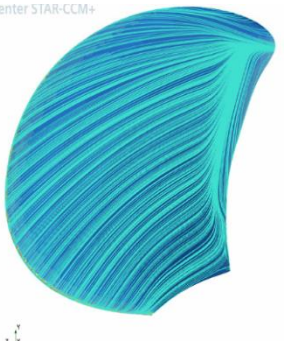 | 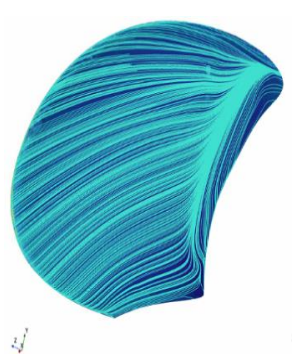 |

**Figure 5: Constrained Streamlines on the Suction Side of the Blade Obtained with the Transition Model at Advance Coefficients J = 0.7985 to J= 1.4594, $Tu$ = 2.0% and $\mu_t$ / $\mu$ =10.0.**

Furthermore, a comparison of the results obtained by the turbulence model with and without using the transition model is conducted with respect to the normalized skin friction coefficient and the pressure on the blade suction side. The normalized skin friction coefficient is defined in Equation (8) as:

$$c_f = \tau_\omega / (0.5 \rho V_{ref}^2) \quad \textbf{(8)}$$

Where, $\tau_w$ is the local wall shear stress over the blade surface and $V_{ref}$ is a non-disturbed on-set velocity at a radius position equal to 0.7R and is defined in Equation (9) as:

$$V_{ref} = \sqrt{(V_A^2 + (0.7R\Omega)^2)} \quad \textbf{(9)}$$

Fig. 6 shows a comparison of the skin friction coefficient obtained by the turbulence model with and without using the transition model. As it can be seen, the results with the turbulence model with the transition model show an increase in the normalized skin friction coefficient contribution at the leading edge which then, decreases in value until the critical Reynolds number $Re_{\theta,C}$ is reached. $Re_{\theta,C}$ increases once again where the position of the transition onset momentum thickness Reynolds number $Re_{\theta t}$ is reached where the transition starts then, it decreases again showing that $Re_{\theta,C}$ is always smaller than $Re_{\theta,t}$ since fluctuations always start before the boundary layer transition.

In addition, a decrease in the pressure coefficient is noticed when the flow regimes change from laminar to turbulent as can be seen in Fig. 7.

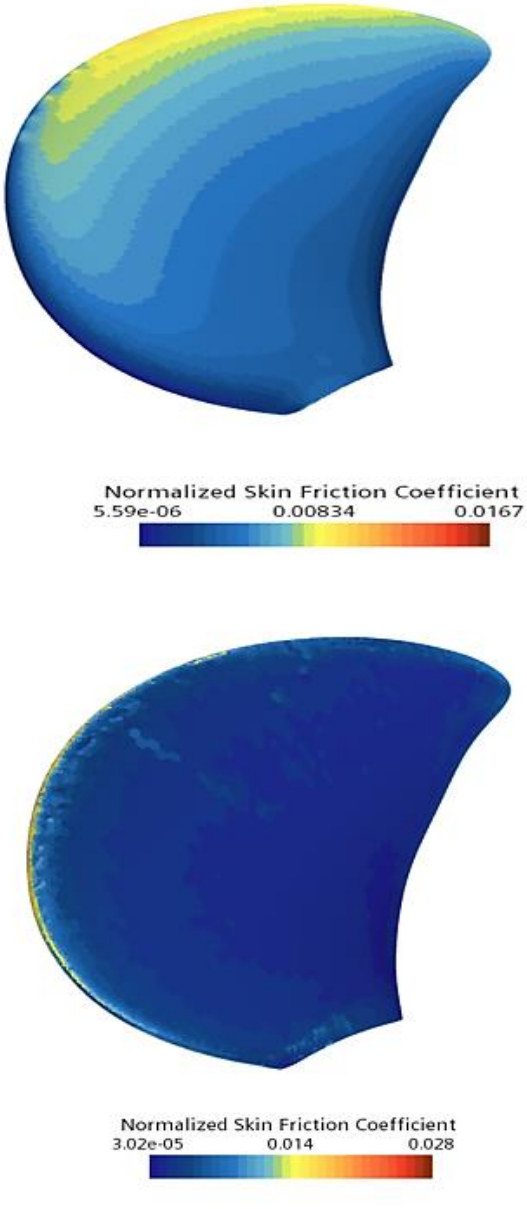


**Figure 6: Normalized Skin Friction Coefficient at J = 1.4594 for Turbulence Model with *Tu* = 1.0% and $\mu_t / \mu$ =1.0 (top). And Transition Model with *Tu* = 2.0% and $\mu_t / \mu$ =10.0 (bottom) at Suction Side.**

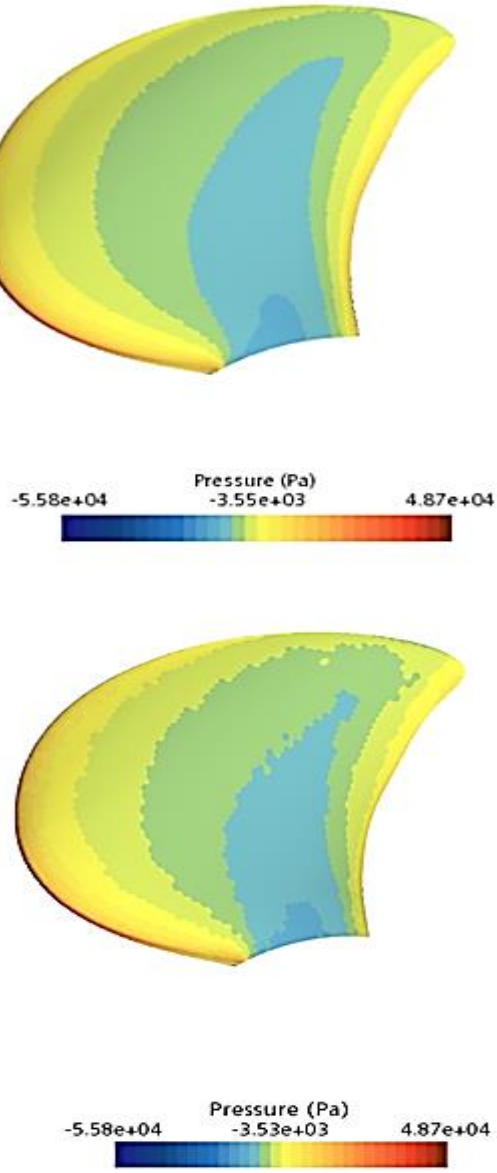


**Figure 7: Pressure Distribution at J = 1.4594 for Turbulence model with Tu = 1.0% and $\mu_t / \mu$ =1.0 (top). and Transition model with Tu = 2.0% and $\mu_t / \mu$ =10.0 (bottom) at suction side.**

## 4 CONCLUSIONS

This paper describes a detailed CFD procedure for simulating the viscous, 3D flow of the well-known PPTC propeller in model scale. The performance characteristics are predicted, and the flow field properties are discussed. The procedure applied considers the possibility of the existence of laminar and transient flow regimes over the propeller blade. The $\gamma - \widetilde{Re}_{\theta t}$ transition model is selected for this criterion with the $k - \omega$ SST turbulence model. This detailed investigation is conducted using the commercially available code STAR-CCM+. The outcomes are compared with published experimental results and the following conclusions is made:

For performing simulations using the transition model, it is important to keep the y+ values for the transition models within the range from 0.1 to 1.0.

The $\gamma - \widetilde{Re}_{\theta t}$ transition model, at model scale, predicts a more accurate value of the open water efficiency than the value predicted by the $k - \omega$ SST turbulence model. In the investigated case, the calculated thrust and torque coefficient values are always slightly higher than experimental results for the $k - \omega$ SST turbulence model, with and without the transition model.

The influence of the inlet turbulence quantities, $Tu$, and $\mu_t / \mu$, on the results obtained by the $k - \omega$ SST turbulence model is small. However, results of the $\gamma - \widetilde{Re}_{\theta t}$ transition model are highly dependent on these turbulence quantities. This can lead to different flow patterns varying from fully laminar to fully turbulent over the blade surface. Due to the high sensitivity of the transition model to turbulence intensity, a high $\mu_t / \mu$ at the inlet of the domain is mandatory to limit the influence of the decay.

The constrained streamlines obtained by the transition model $\gamma - \widetilde{Re}_{\theta t}$ show a more realistic flow pattern than those obtained by the turbulence model $k - \omega$ SST. In addition, the transition model $\gamma - \widetilde{Re}_{\theta t}$ can capture the extent of the laminar and turbulent regions and, the resulting flow pattern is strongly influenced by the inlet turbulence intensity.

## ACKNOWLEDGMENT

The authors are very grateful to Dr. Ginevra Rubino, Ecole Centrale de Nantes, France, for her insight and numerous thoughtful discussions over the transition model development. Additionally, special gratitude thanks to the Maritime Technology Studies Institute (MTSI) for providing their facilities and servers to conduct the simulations and the academic work.

## REFERENCES

Abdel-Maksoud, M. (2003). 'Numerical and Experimental Study of Cavitation Behavior of a Propeller'. In proceeding of the STG sprechtag kavitation, Germany, 11-12.

Baltazar, J., Rijpkema, D., & Campos, J. (2015). 'Viscous flow simulations of propellers in different Reynolds number regimes' . In: Proceedings of the Fourth. International Symposium on Marine Propulsors, Austin, Texas, USA, pp. 446–457.

Baltazar, J., Rijpkema, D., & Falcão de Campos, J. (2018). 'On the use of the $\gamma - \widetilde{Re}_{\theta t}$ transition model for the prediction of the propeller performance at the model scale'. Ocean Engineering, 170 (May), 6–19.

Felicjancik, J., Kowalczyk, S., Felicjancik, K., & Kawecki, K. (2016). 'Numerical Simulations of Hydrodynamic Open-Water Characteristics of a Ship Propeller'. Polish Maritime Research, 23, 16–22.

Gray-Stephens, A., Tezdogan, T., & Day, S. (2020). 'Numerical Modelling of the Nearfield Longitudinal Wake Profiles of a High-Speed Prismatic Planning Hull'. Journal of Marine Science and Engineering, *8*, 516. https://doi.org/10.3390/jmse8070516

Heinke, J. H. (2011). Potsdam Propeller Test Case ( PPTC ) Cavitation Tests with the Model Propeller VP1304. April 1–Report 3752.

Helal, M., Ahmed, T., Banawan, A., & Kotb, M. (2018). 'Numerical prediction of the performance of marine propellers using computational fluid dynamics simulation with transition-sensitive turbulence model'. Alexandria Engineering Journal, 57, 3805-3815

Ingen, J. L. (1956). 'A suggested semi-empirical method for the calculation of boundary layer transition region'. Technische Hogeschool Delft, Vliegtuigbouwkunde, Report VTH-74-95.

Langtry, R. (2006). 'A correlation-based transition model using local variables for unstructured parallelized CFD codes'. PhD thesis, university of Stuttgart, 2006.

Langtry, R., & Menter, F. (2009). 'Correlation-Based Transition Modeling for Unstructured Parallelized Computational Fluid Dynamics Codes'. AIAA Journal

Lardeau, S., Leschziner, M., & Zaki, T. (2012). 'Large Eddy Simulation of Transitional Separated Flow over a Flat Plate and a Compressor Blade'. Flow Turbulence and Combustion, 88.19-44.

Mayle, R., & Schulz, A. (1971). 'The Path to Predicting Bypass Transition'. ASME J. of Turbomachinery, 119, 411–505. https://doi.org/10.1115/96-GT-199

Menter, F. (1994). 'Two-Equation Eddy-Viscosity Turbulence Models for Engineering Applications'. AIAA Journal, 32, 1598–1605.

Menter, F., Kuntz, M., & Langtry, R. (2003). 'Ten years of industrial experience with the SST turbulence model'. International Symposium on Turbulence, Heat and Mass Transfer, 4,625-632.

Menter, F., Smirnov, P., Liu, T., & Avancha, R. (2015). 'A One-Equation Local Correlation-Based Transition Model'. Flow, Turbulence and Combustion, *95*, 583-619. https://doi.org/10.1007/s10494-015-9622-4

Menter, F., Egorov, Y., & Rusch, D. (2006). 'Steady and unsteady flow modeling using the k- k L model. Turbulence Heat and Mass Transfer'. Proceedings of the International Symposium on Turbulence Heat and Mass Transfer, 5, 403-406.

Nakisa, M., Abbasi, M., & Amini, A. M. (2010). ‘of marine propeller hydrodynamic performance in open water via CFD code’. International Conference on Marine Technology (MARTEC 2010).

Narasimha, R. (1957). ‘On the distribution of intermittency in the transition region of a boundary layer’. Journal of Aeronautical Science, 24, 711-712

Rubino, G. (2022). ’Laminar-to-Turbulence Transition Modeling of Incompressible Flows in a RANS Framework for 2D and 3D Configurations’. Fluid mechanics. École centrale de Nantes,2022.

Spalart, P., & Rumsey, C. (2007). ‘Effective Inflow Conditions for Turbulence Models in Aerodynamic Calculations’. AIAA Journal - AIAA J, 45, 2544–2553.

Savill, A. M. (2002). ‘Closure Strategies for Turbulent and Transitional Flows: New Strategies in Modelling By-Pass Transition’.

Tu, T. N. (2019). ‘Numerical simulation of propeller open water characteristics using the RANSE method’. Alexandria Engineering Journal, 58(2), 531–537.

Wang, X., & Walters, K. (2012). ‘Computational Analysis of Marine-Propeller Performance Using Transition-Sensitive Turbulence Modeling’. ASME Journal of Fluids Engineering, *134*, 71107. https://doi.org/10.1115/1.4005729

Watanabe, T., Kawamura, T., Takekoshi, Y., Maeda, M., & Rhee, S. (2003). ‘Simulation of steady and unsteady cavitation on a marine propeller using a RANS CFD code’. in proceedings of the fifth international symposium on cavitation, 2003